UNIVERSITY OF WEST BOHEMIA

Applied and Computational Mechanics 2 (2008) 25–36

Applied and Computational Mechanics

A sandwich bar element for geometric nonlinear thermo-elastic analysis

R. Ďuriš[a,*], J. Murín[b]

[a] *Faculty of Materials Science and Technology, Slovak University of Technology in Bratislava, Paulínska 16, 917 24 Trnava, Slovak Republic*
[b] *Faculty of Electrical Engineering and Information Technology, Slovak University of Technology in Bratislava, Ilkovičova 3, 812 19 Bratislava, Slovak Republic*

Received 31 August 2008; received in revised form 14 October 2008

Abstract

This contribution deals with a two-node straight sandwich composite bar element with constant double symmetric rectangular cross-sectional area. This new bar element (based on the non-linear second-order theory) is intended to perform the non-incremental full geometric non-linear analysis. Stiffness matrix of this composite bar contains transfer constants, which accurately describe polynomial uniaxial variation of the material thermo-physical properties.

In the numerical experiments the weak coupled thermo-structural geometric non-linear problem was solved. Obtained results were compared with several analyses made by ANSYS programme. Findings show good accuracy of this new finite element. The results obtained with this element do not depend on the element mesh density.

Keywords: geometric non-linear analyses, FGM, bar element, sandwich structure

1. Introduction

The composite, sandwich or functionally graded materials (FGMs) are often used in many areas and applications. By mixing two or more appropriate constituents, materials with better properties than single components can be obtained. These materials are characterized by non-homogeneous material properties. Effective numerical analyses of structures made from such materials require homogenisation of uniaxially or spatially variable material properties. Macro-mechanical modelling of these effective material properties of composites is often based on different homogenisation techniques. The simplest mixture rules, which determine average effective material properties, are based on the assumption that the composite material property is the sum of the material properties of each constituent multiplied by its volume fraction [1, 2]. New extended mixture rules [5] are applied in this article, to increase the accuracy of calculation of the effective material properties.

The main aim of this paper is to present new, more effective and accurate truss element with continuous variation of the stiffness along its axis suitable for the solution of geometric and/or physical nonlinear problems.

In the theoretical part of the contribution we describe the equilibrium equations of the new two-node sandwich bar element with variation of thermo-physical material properties. New shape functions of a bar element [3] were used to accurate description of material properties variation along the element length.

*Corresponding author. Tel.: +421 33 5511 601, e-mail: rastislav.duris@stuba.sk.

We consider the straight sandwich bar finite element with constant rectangular cross-sectional area (fig. 1). The composite material of this element arose from two components (matrix and fibre). Longitudinal continuous variation of the fibre and matrix elasticity modulus, thermal expansion coefficient and volume fractions of the constituents can be given in polynomial form in each layer. The homogenisation of the material properties is made for multilayered sandwich bar with constant material properties of middle layer and polynomial variation of elasticity modulus and volume fraction of fibre and matrix at the top/bottom layers. Effect of steady-state temperature field applied in the bar is considered, too [8, 9].

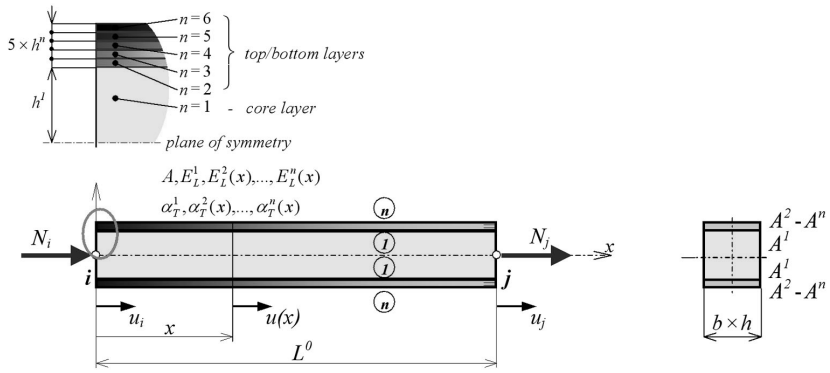

Fig. 1. Double symmetric sandwich bar element with variation of stiffness in initial state

2. Derivation of effective material properties of the symmetric multilayered sandwich bar element

In this contribution we consider sandwich material with continuously variation of elasticity moduli of both, matrix and fibre constituents along the element axis (e.g. caused by non-homogeneous temperature field in a bar). Analogically the thermal expansion coefficient and volume fractions of the constituents vary. The volume fractions and material properties are assumed to be constant through the element depth b and through its height h.

2.1. Variation of material properties and volume fractions of constituents

The uniaxial polynomial variation of fibre elasticity modulus $E_f(x)$ and the matrix elasticity modulus $E_m(x)$ are given as polynomials [5]

$$\begin{aligned} E_f(x) &= E_{fi}\eta_{E_f}(x) = E_{fi}\left(1+\sum_k \eta_{Efk}x^k\right) \\ E_m(x) &= E_{mi}\eta_{E_m}(x) = E_{mi}\left(1+\sum_k \eta_{Emk}x^k\right) \end{aligned} \tag{1}$$

where E_{fi} (E_{mi}) is the fibre (matrix) elastic modulus at node i and $\eta_{E_f}(x)$; $(\eta_{E_m}(x))$ is the polynomial of fibre (matrix) elasticity modulus variation of k order.

The fibre $v_f(x)$ and matrix $v_m(x)$ volume fractions of the constituents are chosen by similar polynomial expressions

$$\begin{aligned} v_f(x) &= 1 - v_m(x) = v_{fi}\eta_{v_f}(x) = v_{fi}\left(1 + \sum_t \eta_{vft}x^t\right) \\ v_m(x) &= 1 - v_f(x) = v_{mi}\eta_{v_m}(x) = v_{mi}\left(1 + \sum_t \eta_{vmt}x^t\right) \end{aligned} \tag{2}$$

where v_{fi} (v_{mi}) is the fibre (matrix) volume fraction at node i and $\eta_{v_f}(x)$ ($\eta_{v_m}(x)$) is the polynomial of fibre (matrix) volume fraction variation of t order.

The effective longitudinal elasticity modulus is then given by

$$E_L(x) = v_f(x)E_f(x) + v_m(x)E_m(x) \tag{3}$$

The bar element with varying stiffness is loaded in linear elastic load state. The effective longitudinal elasticity modulus changes as the polynomial

$$E_L(x) = E_{Li}\eta_{E_L}(x) \tag{4}$$

where $E_{Li} = v_{fi}E_{fi} + (1 - v_{fi}) = v_{fi}E_{fi} + v_{mi}E_{mi}$ is the effective longitudinal elasticity modulus at node i and

$$\eta_{E_L}(x) = 1 + \frac{\eta_{v_f}(x)\eta_{E_f}(x) + \eta_{v_m}(x)\eta_{E_m}(x)}{E_{Li}} = 1 + \sum_{q=1}^{k+t} \eta_{E_Lq}x^q \tag{5}$$

is the relation for effective longitudinal elasticity modulus variation of the bar.

The thermal expansion coefficient of fibre and matrix constituents is considered in the same manner

$$\begin{aligned} \alpha_{Tf}(x) &= \alpha_{Tfi}\eta_{\alpha_{Tf}}(x) = \alpha_{Tfi}\left(1 + \sum_s \eta_{\alpha Tfs}x^s\right) \\ \alpha_{Tm}(x) &= \alpha_{Tmi}\eta_{\alpha_{Tm}}(x) = \alpha_{Tmi}\left(1 + \sum_s \eta_{\alpha Tms}x^s\right) \end{aligned} \tag{6}$$

Order k,t,s of the polynomials (1), (2) and (6) depends on the material properties and the volume fractions variation.

The effective longitudinal thermal expansion coefficient $\alpha_{TL}(x)$ can be calculated using extended Schapery approximation [5] from expression [8, 9]

$$\alpha_{TL}(x) = \frac{v_f(x)\alpha_{Tf}(x)E_f(x) + v_m(x)\alpha_{Tm}(x)E_m(x)}{v_f(x)E_f(x) + v_m(x)E_m(x)} \tag{7}$$

Expression (7) is not polynomial and expansion to Taylor's series is necessary to be used to convert it into polynomial form.

2.2. The effective longitudinal elasticity modulus of a symmetric twelve-layered sandwich bar element

The homogenisation of the material properties is made for 12-layered sandwich bar with double symmetric rectangular constant cross-sectional area A [8]. We assume constant material properties of the middle layer (core) and polynomial variation of the volume fraction of fibre and matrix of the top/bottom layers (fig. 1).

The effective longitudinal elasticity modulus of k-th layer changes according to equation (4)

$$E_L^k(x) = E_{Li}^k \eta_{E_L^k}(x) \tag{8}$$

Index $k \in \langle 1; n = 6 \rangle$ denotes the layer number in the upper/lower symmetrical part of the bar (see fig. 1). Let us define a cross-sectional area ratio of k-th layer

$$r_A^k = \frac{2A^k}{A} \tag{9}$$

where A^k is cross-sectional area of k-th layer and A is total cross-sectional area of the bar.

Then, the homogenized effective longitudinal elasticity modulus of whole element $E_L^H(x)$ in the polynomial form is given by

$$E_L^H(x) = \sum_{k=1}^{n} r_A^k E_L^k(x) = E_{Li}^H \eta_{E_L^H}(x) \tag{10}$$

where E_{Li}^H is the value of homogenized effective longitudinal elasticity modulus at node i and $\eta_{E_L^H}(x)$ is the polynomial of its longitudinal variation.

The homogenized effective longitudinal thermal expansion coefficient of whole element can be calculated from expression

$$\alpha_{TL}^H(x) = \frac{\sum_{k=1}^{n} \alpha_{TL}^k(x) E_L^k(x}{\sum_{k=1}^{n} E_L^k(x)} = \frac{1}{E_L^H(x)} \sum_{k=1}^{n} r_{Ak} \alpha_{TL}^k(x) E_L^k(x) \tag{11}$$

Equation (11) can be transformed to polynomial by Taylor's series to the form

$$\alpha_{TL}^H(x) = \alpha_{TLi}^H \eta_{\alpha_{TL}^H}(x) \tag{12}$$

where α_{TLi}^H is the value of homogenized effective longitudinal thermal expansion coefficient at node$i$ and $\eta_{\alpha_{TL}^H}(x)$ is the polynomial of its longitudinal variation.

3. The bar element with varying stiffness

3.1. Shape functions for axial displacement of the bar element

Using concept published in [7], the elastic kinematical relation between first derivative of the axial displacement function $u(x)$ and axial force $N(x)$ is defined as

$$u'(x) = \frac{N(x)}{AE_L^H(x)} = \frac{N(x)}{AE_{Li}^H \eta_{E_L^H}(x)} \tag{13}$$

We define the second derivative of the transfer function $d_{2E_L^H}(x)$ for pure tension-compression

$$d''_{2E_L^H}(x) = \frac{1}{\eta_{E_L^H}(x)} \tag{14}$$

Then the solution of the differential equation (13), assuming that all element loads are transferred to the nodal points and axial force is constant ($N(x) = N_i = -N_j$), the function of axial displacement is

$$u(x) = u_i - \frac{N_i}{AE^H_{Li}} d'_{2E^H_L}(x) \tag{15}$$

By replacing $x = L^0$ in equation (15) we obtained displacement $u(L^0) = u_j$ and the value of the first derivative of the transfer function $d'_{2E^H_L}(L^0) = d'_{2E^H_L}$, which is called transfer constant for pure tension-compression. Notation of the nodal displacement is in agreement with fig. 1.

Transfer constants can be computed by using simple numerical algorithm published in [3]. The expression relating the axial displacement of an arbitrary point x and the axial displacements of nodal points i and j becomes

$$u(x) = \left(1 - \frac{d'_{2E^H_L}(x)}{d'_{2E^H_L}}\right) u_i + \frac{d'_{2E^H_L}(x)}{d'_{2E^H_L}} u_j = \phi_{1i} u_i + \phi_{1j} u_j \tag{16}$$

Using shape functions ϕ_{1i}, ϕ_{1j} we can derive the stiffness matrix of composite bar that contains transfer constants, which accurately describe the polynomial uniaxial variation of the effective Young's modulus.

3.2. Full geometric non-linear local stiffness matrix of the bar element

For derivation of the new bar element stiffness matrix an approach to evaluation of equilibrium equations published in [4] is used. Thus we can obtain the new geometric non-linear non-incremental formulation of the element stiffness relations. The local FEM equilibrium equations of 2D homogenized bar element [3, 4] has the form

$$\mathbf{K}_u \mathbf{u} = \mathbf{F} \tag{17}$$

where $\mathbf{u} = [u_i, u_j]^T$ is the displacement vector and $\mathbf{F} = [N_i, N_j]^T$ is the load vector. By implementation of the shape functions with transfer functions and constants we get the non-linear stiffness matrix $\mathbf{K}_u$ in the form

$$\mathbf{K}_u = \frac{AE^H_{Li}}{d'_{2E^H_L}} \left[1 + \frac{3}{2}(\lambda - 1)\frac{\overline{d'_{2E^H_L}}}{(d'_{2E^H_L})^2} + \frac{1}{2}(\lambda - 1)^2 \frac{\overline{\overline{d'_{2E^H_L}}}}{(d'_{2E^H_L})^3}\right] \begin{bmatrix} 1 & -1 \\ -1 & 1 \end{bmatrix} \tag{18}$$

where $\overline{d'_{2E^H_L}} = \int_0^{L^0} \left(d''_{2E^H_L}(x)\right)^2 \mathrm{d}x$, $\overline{\overline{d'_{2E^H_L}}} = \int_0^{L^0} \left(d''_{2E^H_L}(x)\right)^3 \mathrm{d}x$ are the transfer constants for homogenized effective longitudinal elasticity modulus (10) and $\lambda = (u_j - u_i)/L^0 + 1$ is stretching of the bar.

The axial force in the bar element can be calculated using the formulae

$$N_i = -\frac{AE^H_{Li}}{d'_{2E^H_L}} \left[1 + \frac{3}{2}(\lambda - 1)\frac{\overline{d'_{2E^H_L}}}{(d'_{2E^H_L})^2} + \frac{1}{2}(\lambda - 1)^2 \frac{\overline{\overline{d'_{2E^H_L}}}}{(d'_{2E^H_L})^3}\right] (\lambda - 1) L^0 \tag{19}$$

The resulting system of non-linear equations (17) is usually solved by using Newton-Raphson method. In this solution process, the full non-linear tangent stiffness matrix was expressed by

$$\mathbf{K}_T = \frac{\partial \mathbf{F}}{\partial \mathbf{u}} = \frac{AE^H_{Li}}{d'_{2E^H_L}} \left[1 + 3(\lambda - 1)\frac{\overline{d'_{2E^H_L}}}{(d'_{2E^H_L})^2} + \frac{3}{2}(\lambda - 1)^2 \frac{\overline{\overline{d'_{2E^H_L}}}}{(d'_{2E^H_L})^3}\right] \begin{bmatrix} 1 & -1 \\ -1 & 1 \end{bmatrix}. \tag{20}$$

Local stiffness matrices can be transformed to global coordinate system by using standard transformation rules.

3.3. Influence of temperature field

In the case, when the temperature load is changing along the bar element length only, the effective thermal nodal forces are derived as follows [6]

$$\begin{bmatrix} F_i^{th} \\ F_j^{th} \end{bmatrix} = \begin{bmatrix} -1 \\ 1 \end{bmatrix} \frac{E_{Li}^H A \alpha_{TLi}^H \Delta T_i}{d'_{2E_L^H}} \int_0^{L^0} \eta_{\alpha\Delta T}(x)\,\mathrm{d}x \tag{21}$$

where $\Delta T_i = T_i - T_{ref}$ is temperature difference at node i with respect to reference temperature, $\eta_{\alpha\Delta T}(x)$ is polynomial represented by expression

$$\eta_{\alpha\Delta T}(x) = \eta_{\alpha_{TL}^H}(x)\eta_{\Delta T}(x) \tag{22}$$

and $\eta_{\Delta T}(x) = \frac{T(x)-T_{ref}}{T_i-T_{ref}}$ is the polynomial of the varying temperature field.

Thermal strain $\varepsilon_0(x)$ can be calculated using the equation

$$\varepsilon_0(x) = \alpha_{TL}^H(x)(T(x) - T_{ref}) = \alpha_{TLi}^H \Delta T_i \eta_{\alpha_{TL}^H}(x)\eta_{\Delta T}(x) = \alpha_{TLi}^H \Delta T_i \eta_{\alpha\Delta T}(x) \tag{23}$$

Deformation of the bar due to thermal loading is

$$\Delta u_T = \int_{(L^0)} \varepsilon_0(x)\,\mathrm{d}x = \alpha_{TLi}^H \Delta T_i \int_{(L^0)} \eta_{\alpha\Delta T}(x)\,\mathrm{d}x \tag{24}$$

For inclusion of thermal forces it is sufficient to change the right side of (17) to

$$\mathbf{F} = \begin{bmatrix} N_i \\ N_j \end{bmatrix} + \begin{bmatrix} F_i^{th} \\ F_j^{th} \end{bmatrix} \tag{25}$$

3.4. Normal stress caused by structural axial loading

The expression for calculation of the effective longitudinal strain we get from derivation of equation (16) in the form

$$\varepsilon(x) = \frac{u_j - u_i}{\eta_{E_L^H}(x) d'_{2E_L^H}} \tag{26}$$

The effective normal stress in the homogenized bar is then

$$\sigma(x) = \varepsilon(x) E_L^H(x) \tag{27}$$

Real stress in the k-th layer is

$$\sigma^k(x) = \varepsilon(x) E_L^k(x) \tag{28}$$

3.5. Thermal stress

The thermal stresses in the bar are caused by different thermal expansion coefficient of individual layers. Thermal stress in k-th layer can be calculated from [8, 9]

$$\sigma_{th}^k(x) = (\alpha_{TL}^H(x) - \alpha_{TL}^k(x))(T(x) - T_{ref}) E_L^k(x) \tag{29}$$

3.6. Total strain and stress

Total normal stress in k-th layer is equal to the sum of structural and thermal stress

$$\sigma^k_{total}(x) = \sigma^k_L(x) + \sigma^k_{th}(x) \tag{30}$$

The total effective longitudinal strain we get by modification of effective structural strain (26) to the form [8, 9]

$$\varepsilon_{total}(x) = \frac{(u_j - u_i) - \Delta u_T}{\eta_{E^H_L}(x) d'_{2E^H_L}} \tag{31}$$

4. Numerical experiments

To show the structural behaviour of new element, we consider 12-layered two-node sandwich bar with constant cross-sectional area (see fig. 1). Layout and geometry of layers is symmetric to neutral plane. Material of layers consists of two components: NiFe denoted as the *matrix* (index m) and Tungsten named as the *fibre* (index f). Geometry and material parameters for the bar chosen for numerical examples are summarized in tab. 1. In numerical examples the constant linear elastic material properties of constituents are assumed ($E_f = \text{const.}$ and $E_m = \text{const.}$). Material of the middle layer (core layer denoted as 1) is the pure matrix with constant Young's modulus E_m. Symmetric pairs of layers $k = \langle 2, \ldots, 6 \rangle$ were fabricated by non-uniform mixing of both matrix and fibre components. Volume fraction of fibre is constant along the width and height of each layer, but it changes linearly along the layer length i.e. mechanical properties vary along the width and length of the specimen. This longitudinal variation of volume fraction of fibre (matrix) in k-th layer is described by equation (2). At node i the volume fractions of fibre are different in each layer and at node j this ratio is considered to be constant in all layers.

Table 1. Elastic moduli of the constituents and the specimen proportions

material properties		
Tungsten (*fibres*)	elasticity modulus	$E_m = 400\,\text{GPa}$
	thermal expansion coefficient	$\alpha_{Tf} = 5.3 \cdot 10^{-6}\,\text{K}^{-1}$
NiFe (*matrix*)	elasticity modulus	$E_f = 255\,\text{GPa}$
	thermal expansion coefficient	$\alpha_{Tf} = 1.5 \cdot 10^{-5}\,\text{K}^{-1}$
geometrical parameters		
specimen length	$L^0 = 0.1\,\text{m}$	
specimen width	$b = 0.01\,\text{m}$	
specimen height	$h = 0.01\,\text{m}$	
total number of layers (incl. core)	$2n = 12\ (2 \cdot 6)$	
initial angle	$\alpha^0 = 7°$	
cross-sectional area	$A = 0.000\,1\,\text{m}^2$	
cross-sectional area of 1^{st} layer	$A^1 = 0.000\,04\,\text{m}^2$	
cross-sectional area of k^{th} layer	$A^k = 0.000\,002\,\text{m}^2$	
total thickness of face layers	$t = 0.001\,\text{m}$	
thickness of 1^{st} layer	$h^1 = 0.004\ \text{m}$	
thickness of k^{th} layer	$h^k = 0.000\,2\,\text{m}$	

In the numerical experiments the accuracy and efficiency of the new non-incremental geometric non-linear bar element equations with varying of effective material properties were examined. As a typical example of geometrically non-linear behaviour the three-hinge mechanism was chosen and analysed (fig. 2).

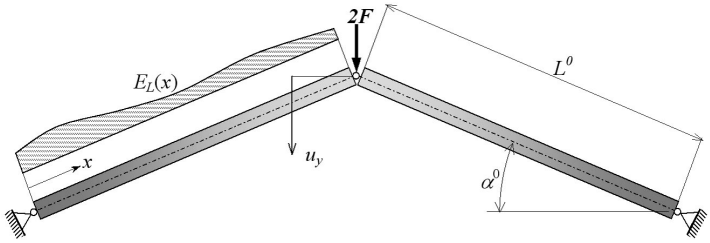

Fig. 2. Von Mises bar structure

Volume fraction of the components varies linearly along the k-th layer length in accordance with (2)

$$\nu_f^k(x) = 1 - \nu_m^k(x) = \nu_{fi}^k(1 + \eta_{\nu f1}^k x) \qquad k \in \langle 2, \ldots, 6 \rangle$$

List of $\nu_{fi}^k, \eta_{\nu f1}^k$ parameters is given in tab. 2.

Table 2. Polynomial variation of fibre volume fraction along the x axis of the element

layer k	1	2	3	4	5	6
ν_{fi}^k	0	0.6	0.7	0.8	0.9	1.0
$\eta_{\nu f1}^k$	0	$-3/0.6$	$-4/0.7$	$-5/0.8$	$-6/0.9$	$-7/1.0$

Using equation (3) we can get the effective longitudinal elasticity modulus of the individual layers in the form

$E_L^1(x) = 2.55 \cdot 10^{11}$ [Pa] $\qquad E_L^2(x) = (3.42 - 4.35x) \cdot 10^{11}$ [Pa]

$E_L^3(x) = (3.56 - 5.80x) \cdot 10^{11}$ [Pa] $\qquad E_L^4(x) = (3.71 - 7.25x) \cdot 10^{11}$ [Pa]

$E_L^5(x) = (3.85 - 8.70x) \cdot 10^{11}$ [Pa] $\qquad E_L^6(x) = (4.00 - 1.01x) \cdot 10^{11}$ [Pa]

The effective elasticity modulus of the homogenized sandwich calculated by expression (10) is

$$E_L^H(x) = (2.782 - 1.45x) \cdot 10^{11} \text{ [Pa]}$$

All effective elasticity moduli are shown in fig. 3.

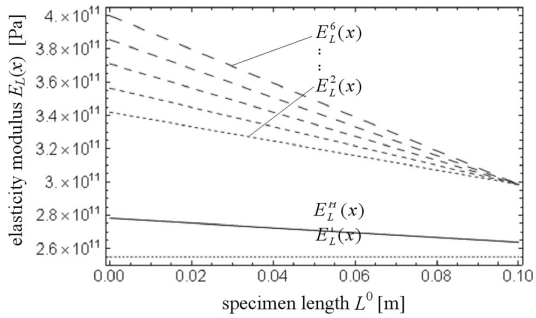

Fig. 3. Variations of all effective longitudinal elasticity moduli

Also thermal expansion coefficients of individual layers were obtained by expression (7)

$$\alpha_{TL}^{1}(x) = 1.5 \cdot 10^{-5}\,[\mathrm{K}^{-1}] \qquad \alpha_{TL}^{2}(x) = \frac{1.5686 \cdot 10^{-5}}{0.78620 - x} - 1.1758 \cdot 10^{-5}\,[\mathrm{K}^{-1}]$$

$$\alpha_{TL}^{3}(x) = \frac{1.1764 \cdot 10^{-5}}{0.61465 - x} - 1.1758 \cdot 10^{-5}\,[\mathrm{K}^{-1}] \qquad \alpha_{TL}^{4}(x) = \frac{9.4116 \cdot 10^{-6}}{0.51172 - x} - 1.1758 \cdot 10^{-5}\,[\mathrm{K}^{-1}]$$

$$\alpha_{TL}^{5}(x) = \frac{7.8430 \cdot 10^{-6}}{0.44310 - x} - 1.1758 \cdot 10^{-5}\,[\mathrm{K}^{-1}] \qquad \alpha_{TL}^{6}(x) = \frac{6.7226 \cdot 10^{-6}}{039408 - x} - 1.1758 \cdot 10^{-5}\,[\mathrm{K}^{-1}]$$

The effective thermal expansion coefficient of the homogenized sandwich was calculated by expression (11) and transformed to the polynomial form

$$\begin{aligned} \alpha_{TL}^{H}(x) \;=\; & 1.276\,8 \cdot 10^{-5} + 1.278\,3 \cdot 10^{-5} x + 6.662\,9 \cdot 10^{-6} x^2 + 3.472 \cdot 10^{-6} x^3 + \\ & + 1.81 \cdot 10^{-6} x^4 + 9.434\,1 \cdot 10^{-7} x^5 + 4.917\,1 \cdot 10^{-7} x^6\,[\mathrm{K}^{-1}] \end{aligned}$$

All thermal expansion coefficients are shown in fig. 4.

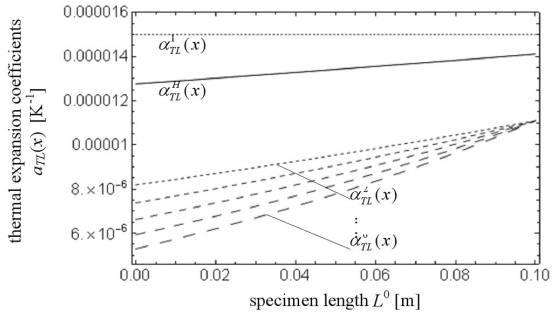

Fig. 4. Variations of all effective longitudinal thermal expansion coefficients

To compare and evaluate the numerical accuracy of new element and extended mixture rules, four different models were used — three one-dimensional and one three-dimensional model:

- Beam model divided into 20 BEAM3 elements (based on Hermite shape functions) in ANSYS programme
- Beam model meshed to 20 BEAM188 elements (linear isoparametric shape functions) in ANSYS programme
- Solid model with very fine mesh (10 080 SOLID45 elements) in ANSYS programme
- To examine the accuracy of the new bar element, an individual code in MATHEMATICA programme was written. Only single our new finite element was used for solution of the chosen problem.

The results obtained by this new element were compared with the beam and solid model analysis results performed by ANSYS.

In all solutions steady-state temperature field was considered as an additional loading described by relation

$$T(x) = 30(1 - 2x + 4x^2)\,[^{\circ}\mathrm{C}]$$

The reference temperature $T_{ref} = 0\,^{\circ}\mathrm{C}$.

We used the effective longitudinal material properties of individual layer in solid analysis in ANSYS and the homogenized effective material properties of sandwich were used in the new bar element (MATHEMATICA) and for the ANSYS beam models, respectively.

Results of both, the ANSYS and the new bar element solutions are presented in the following graphs. The first graph shows relation between common hinge displacement vs. global reaction (fig. 5). The second graph shows relation between common hinge displacement vs. axial force (fig. 6).

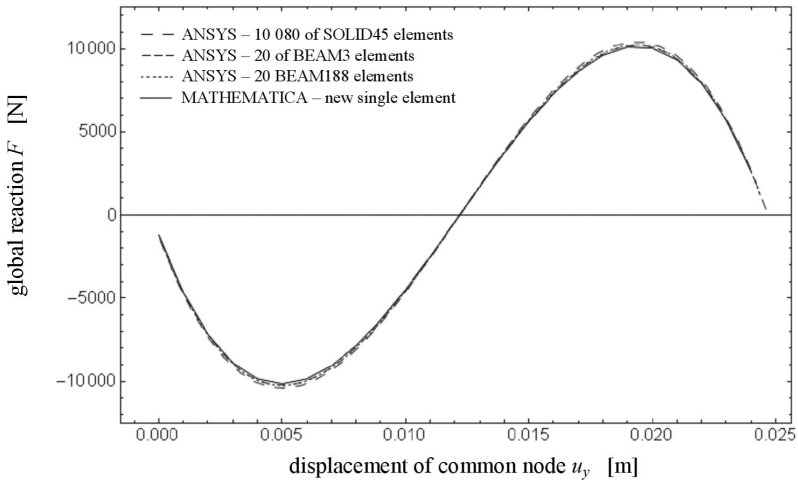

Fig. 5. Common hinge displacement vs. global reaction

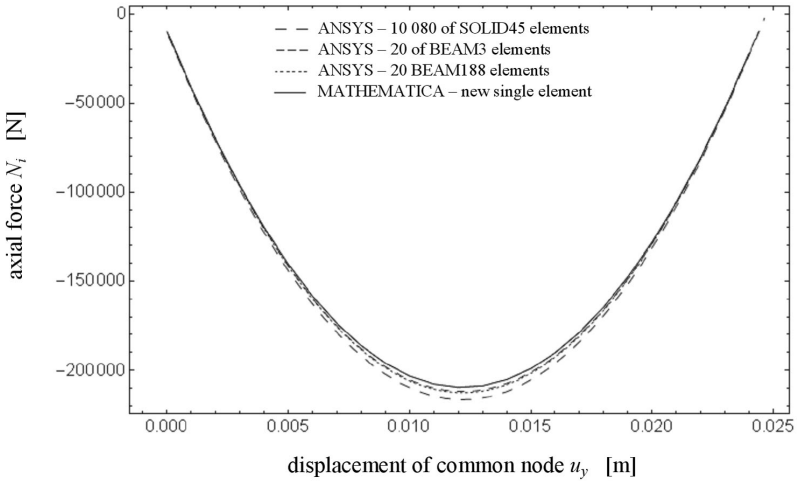

Fig. 6. Common hinge displacement vs. axial force

Total stresses in the new bar element calculated by using (30) are shown in fig. 7. Both results obtained from new single bar element and ANSYS solid analysis are presented.

Maximum intensity of both axial forces and absolute value of global reaction forces obtained from numerical analyses are shown in the tab. 3. In the tab. 4 the absolute percentage differences of the new bar solutions comparing to the ANSYS reference solutions are presented.

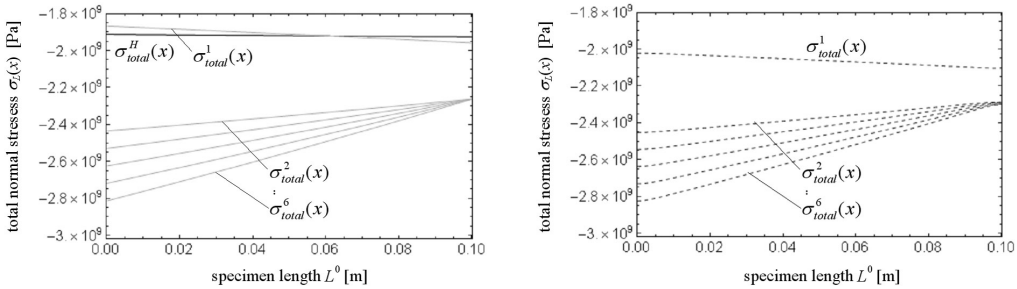

Fig. 7. Distribution of normal stresses in individual layers and homogenized normal stress a) in new bar element, b) results of ANSYS solid analysis

Table 3. Results of maximum forces for the new bar and ANSYS solutions

axial force N [N]			
new bar element 1 element	ANSYS – BEAM188 20 elements	ANSYS – BEAM3 20 elements	ANSYS – SOLID45 20 elements
$-209\,605$	$-212\,626$	$-211\,868$	$-216\,565$
global reaction $\|F\|$ [N]			
new bar element 1 element	ANSYS – BEAM188 20 elements	ANSYS – BEAM3 20 elements	ANSYS – SOLID45 20 elements
10 148.3	10 248	10 223.5	10 420.9

Table 4. Percentage differences between the new bar analysis and ANSYS solutions

difference of axial force N			difference of global reaction F		
$\frac{new\ bar - ANSYS\ BEAM188}{ANSYS\ BEAM188}$	$\frac{new\ bar - ANSYS\ BEAM3}{ANSYS\ BEAM3}$	$\frac{new\ bar - ANSYS\ SOLID45}{ANSYS\ SOLID45}$	$\frac{new\ bar - ANSYS\ BEAM188}{ANSYS\ BEAM188}$	$\frac{new\ bar - ANSYS\ BEAM3}{ANSYS\ BEAM3}$	$\frac{new\ bar - ANSYS\ SOLID45}{ANSYS\ SOLID45}$
1.42 %	1.07 %	3.21 %	0.97 %	0.74 %	2.62 %

Table 5. Compresive stresses in middle of k-th layer in load substep $\alpha^t = 0°$ (maximum of stresses in the bar)

node	n^{th} layer:	axial stress in k-th layer $\sigma^n_{i(j)}$ [MPa]					
		1	2	3	4	5	6
i	new element	$-1\,867.83$	$-2\,435.26$	$-2\,529.82$	$-2\,624.40$	$-2\,718.97$	$-28\,13.54$
	ANSYS solid	$-2\,021.35$	$-2\,453.76$	$-2\,543.79$	$-2\,637.04$	$-2\,730.51$	$-2\,823.51$
j	new element	$-1\,958.20$	$-2\,262.92$				
	ANSYS solid	$-2\,102.99$	$-2\,288.49$	$-2\,289.59$	$-2\,293.26$	$-2\,296.74$	$-2\,299.26$

Tab. 5 shows results of maximum axial stresses in the middle of each layer obtained by using one new bar element and ANSYS solid analysis. Presented results correspond to the load substep where local axis x of the bar is identical with global x axis. Effective axial stress in the bar with homogenised material properties is in this state $\sigma^H_L = -2.096\,05 \cdot 10^9$ Pa.

5. Conclusion

The results of numerical experiments are presented in this contribution using the above mentioned mixture rules. All variations of material properties are included into the bar element stiffness matrix through transfer constants. The effective material properties were calculated by extended mixture rules and by the laminate theory. New finite bar element can also be used in the case when the effective material properties were obtained by other homogenization technique. Presented bar finite element is applicable in problems with large deformations but small strains.

The obtained results are compared with solid analysis in the ANSYS simulation programme. Findings show good accuracy and effectiveness of this new finite element and new homogenization procedure. The difference between ANSYS solid analysis and new element results are less than 2.62 % for the global reaction and 3.21 % for axial force. The results obtained with this element do not depend on the mesh density.

Acknowledgements

This work was supported by the Slovak Grant Agency, grant VEGA 1/4122/07 and Ministry of Education of the Slovak Republic, grant AV-4/0102/06. This support is gratefully acknowledged.

References

[1] H. Altenbach, J. Altenbach, W. Kissing, Mechanics of Composite Structural Elements, Springer-Verlag, 2003.

[2] A. Chakraborty, S. Gopalakrishnan, J. N. Reddy, A new beam finite element for the analysis of functionally graded materials, International Journal of Mechanical Sciences 45 (3) (2003) 519–539.

[3] V. Kutiš, Beam element with variation of cross-section, which satisfies all local and global equilibrium conditions, Ph.D. Thesis, Department of Mechanics, FEI STU (Slovak University of Technology), Bratislava, 2001.

[4] J. Murín, Implicit non-incremental FEM equations for non-linear continuum. Strojnícky časopis 52 (3) (2001).

[5] J. Murín, V. Kutiš, Improved mixture rules for the composite (FGM's) sandwich beam finite element, In: 9th International Conference on Computational Plasticity COMPLAS IX, Fundamentational and Applications Part 2, Barcelona, 2007, 647–650.

[6] J. Murín, V. Kutiš, M. Masný, An effective solution of electro-thermo-structural problem of uniaxially graded material, Structural Engineering and Mechanics 28 (6) (2008) 695–714.

[7] H. Rubin, Bautechnik, Ernst and Sohn, 1999.

[8] J. Murín, V. Kutiš, M. Masný, An Effective Multiphysical Functionally Graded Material Beam-Link Finite Element with Transversal Symmetric and Longitudinal Continuous Variation of Material Properties. In: Proceedings of the Ninth International Conference on Computational Structures Technology, Athens, Greece, Civil-Comp-Press, 2008.

[9] J. Murín, V. Kutiš, An effective thermo-elastic composite (FGMs) multilayered sandwich beam finite element. Manuscript of paper sent for publishing in Structural Engineering and Mechanics.